ISSN 0208-7774 TRIBOLOGIA 2/2019 p. 143–149
DOI: 10.5604/01.3001.0013.4165

**Grzegorz ZAJĄC*, Maciej MICHNEJ****

# FATIGUE STRENGTH IMPROVEMENT OF STEEL ROLLERS IN CONVEYOR BELTS WHEN USING SHOT PEENING

# POPRAWA WYTRZYMAŁOŚCI ZMĘCZENIOWEJ KRĄŻNIKÓW STALOWYCH PRZENOŚNIKÓW TAŚMOWYCH PRZY STOSOWANIU NAGNIATANIA DYNAMICZNEGO

**Key words:** conveyor belts, rollers, fatigue strength.

**Abstract**

Numerous factors influence the tribological wear of steel rollers used in conveyor belts. The difficulty in precise determination of these factors results from, among others, a complex and not completely explored wear mechanism. Corrosive and fatigue damages of conveyor belt rollers start mainly on the surface. The present article describes studies on the influence of processing technology of the roller surface by means of the shot peening method in the context of fatigue strength improvement. Compressive stresses formed due to shot peening reach the maximum value just below the roller surface. The values of compressive stresses reach about half of the proof stress of the steel from which they are made. In results of the carried out experimental model tests, it was found that it is possible to significantly improve the properties of the top surface layer of the roller surface, and especially to increase fatigue strength, fatigue corrosion resistance, resistance to cracking caused by stress corrosion, and the like.

**Słowa kluczowe:** przenośniki taśmowe, krążniki, wytrzymałość zmęczeniowa.

**Streszczenie**

Na zużycie tribologiczne krążników stosowanych w przenośnikach taśmowych ma wpływ bardzo wiele czynników. Trudność w określeniu dokładnej liczby czynników wynika między innymi ze złożonego i nie do końca zbadanego mechanizmu zużywania. Uszkodzenia krążników przenośników taśmowych o charakterze korozyjnym i zmęczeniowym zaczynają się głównie na powierzchni płaszcza. W niniejszym artykule przedstawiono badania wpływu technologii obróbki powierzchni płaszczy krążników metodą nagniatania dynamicznego w kontekście poprawy wytrzymałości zmęczeniowej. Naprężenia własne ściskające wytworzone wskutek nagniatania dynamicznego osiągają maksymalną wartość tuż pod powierzchnią płaszcza krążnika. Wartości naprężeń własnych ściskających osiągają około połowę umownej granicy plastyczności stali, z której są one wykonane. W wyniku przeprowadzonych modelowych badań doświadczalnych stwierdzono możliwość znaczącej poprawy własności warstwy wierzchniej płaszczy krążników, a w szczególności podniesienie wytrzymałości zmęczeniowej, odporności na korozję zmęczeniową, odporności na pękanie w wyniku korozji naprężeniowej itp.

## INTRODUCTION

**Figure 1** presents a reference plain steel roller for conveyor belts made of S235 steel. The roller surface is made of steel pipe of 51 mm, 63.5 mm, 88.9 mm, 108 mm, 133 mm, and 159 mm in diameter. The roller axis set in rolling bearings may have different types of finish. The rollers can be prepared in different variants of anticorrosive surface protection (with undercoat, powder paint or galvanized). The tribological wear process of the rollers used in conveyor belts can be influenced by many various factors. The difficulty in precise determination of these factors results from, among others, a complex and not completely explored wear mechanism. The most

* ORCID: 0000-0003-3326-1154. Cracow University of Technology, Institute of Rail Vehicles, Jana Pawła II 37 Avenue, 31-864 Cracow, Poland, tel. 12 374 33 10, e-mail: m-8@mech.pk.edu.pl.
** ORCID: 0000-0003-0030-1973. Cracow University of Technology, Institute of Rail Vehicles, Jana Pawła II 37 Avenue, 31-864 Cracow, Poland, tel. 12 374 33 10, e-mail: m-8@mech.pk.edu.pl.

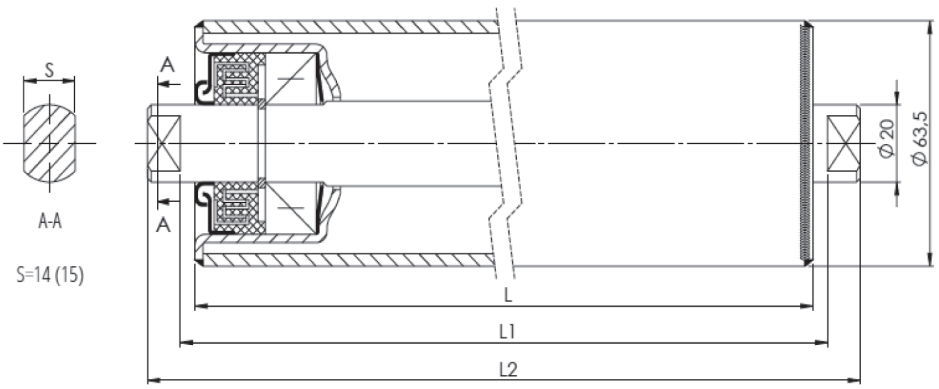


**Fig. 1. General view of the reference plain steel roller for conveyor belts**
Rys. 1. Widok ogólny referencyjnego krążnika stalowego gładkiego do przenośników taśmowych

division of factors influencing the wear in publications are those connected with the following:
– The relative displacement conditions of the combined elements,
– Surrounding conditions, and
– The properties of the materials.

The biggest influence on the wear process is the structure of the junction of the roller surface and the belt of the conveyor as a tribological system and the surroundings of the node. In the exploitation conditions, the roller is subjected to extortions such as a movement of a given amplitude, frequency, and load. The impact of the surrounding includes temperature, humidity, and oxygen access. The structures of the junction node are the touching top layers, wear products, and the mechanical and tribological properties of the structure elements and the relations between them.

## SHOT PEENING TECHNOLOGY

Based on analysis, the technology of shot peening was chosen for further studies of the chosen technological processes that make it possible to improve the mechanical properties of the top layer. This is due to low costs and the possibility of simultaneous performing of the operation connected with cleaning of the roller surface before providing anticorrosive protection and its strengthening.

Shot peening technology is an abrasive blasting process which became popular about 130 years ago. At first, it was used to clean and remove scales from the machine parts, Now, it is used to increase such parameters of the machine parts as fatigue strength, wear, and corrosion cracking **[L. 1, 2]**.

Shot peening is one of the methods used for surface strengthening of machine parts. It consists in submitting the element surface to the action of a shot flux thrown at the speed from 40 to 150m/s, depending on the processing parameters. The results of such surface treatment are plastic deformations and compressive stresses formed in the top layer of the processed element. The advantage of shot peening is the possibility of using this way of processing in surfaces of complex shapes **[L. 3]**.

The most important advantages of this process are the following:
– Broken contact of the burnished element with the processed surface,
– Variable force values during processing and the small load of the machine tool – workpiece tool system elements, and
– Very good heat dissipation from the treatment zone.

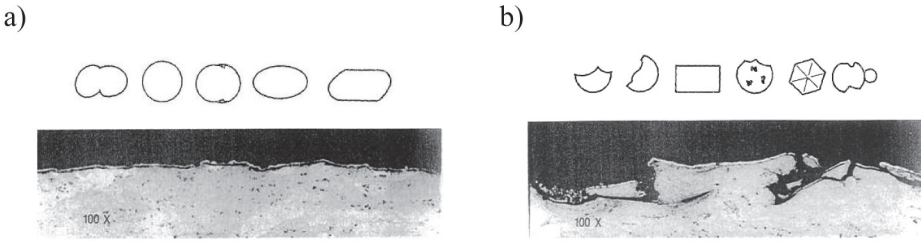


**Fig. 2. Shape of shot grains: a) acceptable, b) unacceptable and appearance of surfaces after their application to the treatment [L. 3]**
Rys. 2. Kształty ziaren śrutu: a) dopuszczalne, b) niedopuszczalne oraz wygląd powierzchni po zastosowaniu ich do obróbki **[L. 3]**

In shot peening, both mechanical and pneumatic devices are used. In recent years, laser shot peening devices have been introduced into the production practice **[L. 4, 5]**. In the mechanical devices, the kinetic energy of the shot is obtained by means of rotor blades, while air pressure is obviously used in pneumatic peening. In the laser shot peening process, coherent light impulses are used to induce plastic deformations. The depth of the layer strengthened by this method is over 1 mm, which is not achievable in the case of traditional shot peening. The following shot types are applied: spherical shapes are made from casting or cylindrical ones cut from wire. Among spherical shot, the following can be distinguished: cast iron, cast steel, and glass. Cylindrical shots are mostly made of steel wire used for making springs. For shot peening of machine parts, shot is also made of aluminium, titanium, ceramics, plastics, nut shells, and hard fruit seeds. Acceptable and unacceptable shapes of the shot grains and the appearance of the surface treated by them are shown in **Fig. 2**.

## LABORATORY TRIBOLOGICAL TESTS OF PLAIN STEEL ROLLER SAMPLES MADE OF S235 STEEL

Tested samples were made of S235 steel in agreement with the guidelines included in the instruction of T-05 stand and research methodology worked out by the authors. Geometrical and technological requirements, according to which the samples had been prepared, are presented in **Figs. 3** and **4**.

**Figure 3** shows the shape and requirements according to which the samples of S235 material (used in the analysed plain steel rollers) were made. **Figure 4** presents a sample design in the cuboid shape and made of S235 steel for testing concentrated contact.

After initial validation of the results, the conditions in which the samples had been prepared were quantified and modified. Modifications were based on additional conditioning of the samples in a container filled with sand. After 24 hours of conditioning, the sand covered samples were subjected to tribological wear tests without any other forms of impact on the friction surface (not including atmospheric conditions), and this procedure produced reliable results. It was assumed that such a simulation of a roller's working conditions is more reliable and better corresponds to the actual exploitation conditions, that is, among others, high dustiness and the presence of micro-particles in the atmosphere. Moreover, due to the introduction of "residual quartz," the wear of adhesive character was limited, which can be considered to be of little importance in the actual friction node. Considering forms of tribological wear, the principle should be taken into account that the increase of the hardness of the materials in a friction contact lowers adhesive wear intensity. In reference to the developed technology, it was stated that the increase of roller's surface hardness is one of the main effects of applying this technology which the results of this study confirm.

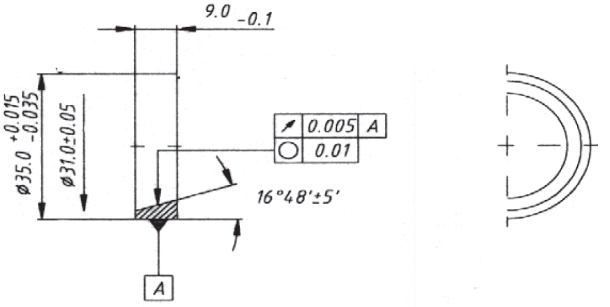


**Fig. 3. Rim pattern (countertop) made of S235 material**
Rys. 3. Schemat obręczy (przeciwpróbki) wykonanej z materiału S235

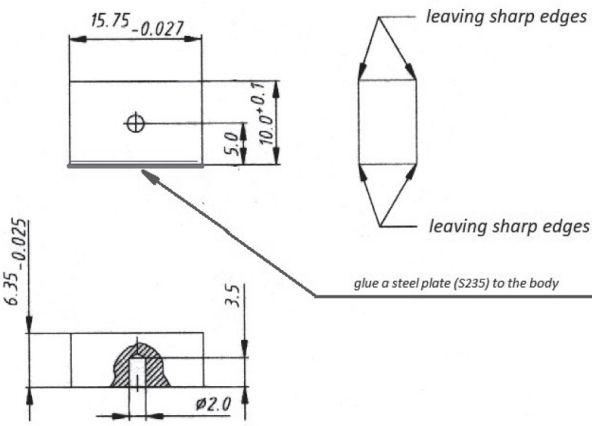


**Fig. 4. Sample design made of S235 steel**
Rys. 4. Schemat próbki wykonanej ze stali S235

Volumetric wear of $Z_v$ sample was calculated from (1):

$$Z_v = \frac{D_t^2 \cdot l}{8}[2\arcsin\frac{b}{D_t} - \sin(2\arcsin\frac{b}{D_t})]\,[mm^3] \qquad (1)$$

where
$D_t$ – test rim diameter [mm],
$l$ – test block width [mm],
$b$ – mean width of friction track [mm].

Mass wear for a sample of concentrated contact was calculated according to the following dependency (2):

$$Z_m = Z_v \cdot \rho_r \quad [\mathrm{g}] \qquad (2)$$

where
$\rho_r$ – sample material density [g*mm$^{-3}$].

**Table 1** lists average levels of volumetric and bulk samples after tribological tests in the T-05 stand.

**Figure 5** shows the values of volume loss measured during tribological tests.

**Table 1. A summary of the average levels of volumetric and bulk wear of tribologically tested T-05 samples**
Tabela 1. Zestawienie średnioważonych wartości zużycia objętościowego i masowego próbek po badaniu tribologicznym na stanowisku T-05

| No. | Sample material | Symbol and type of counterspecimen | Load [N] | Nominal number of cycles | Friction rate [m/s] ±0,1 | Volume loss [mm$^3$] |
|---|---|---|---|---|---|---|
| 1 | S235/S235 | S235_T0 | 175 | 3000 | 1.09 | 2.769234 |
| 2 | S235/S235 | S235_T0 | 175 | 3000 | 1.09 | 3.068348 |
| 3 | S235/S235 | S235_T0 | 175 | 3000 | 1.09 | 2.905807 |
| 4 | S235/S235 | S235_T0,7 | 175 | 3000 | 1.09 | 2.123425 |
| 5 | S235/S235 | S235_T0,7 | 175 | 3000 | 1.09 | 2.268472 |
| 6 | S235/S235 | S235_T0,7 | 175 | 3000 | 1.09 | 2.293237 |
| 7 | S235/S235 | S235_T0,9 | 175 | 3000 | 1.09 | 2.231167 |
| 8 | S235/S235 | S235_T0,9 | 175 | 3000 | 1.09 | 2.092683 |
| 9 | S235/S235 | S235_T0,9 | 175 | 3000 | 1.09 | 2.277484 |

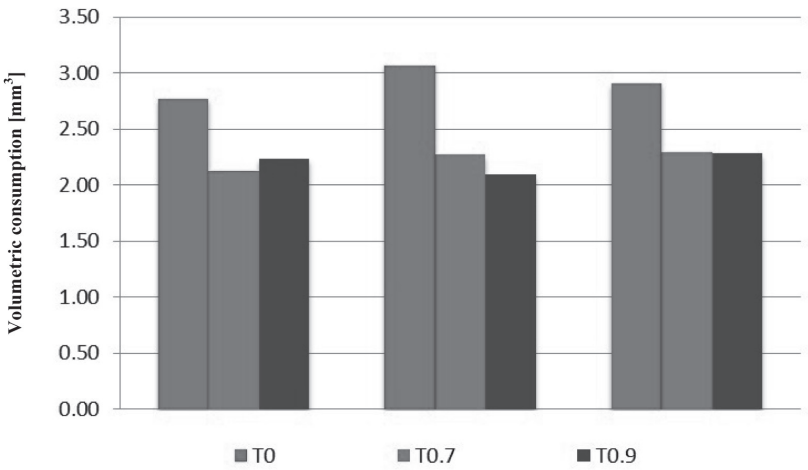


**Fig. 5. Histograms of values of tested samples T0, T0.7, T0.9 friction rate 1.1 [m/s], load 175 [N]**
Rys. 5. Histogram wartości zużycia objętościowego badanych próbek T0, T0.7, T0.9 prędkość sił tarcia 1.1 [m/s], obciążenie 175 [N]

**Figures 6** and **7** present selected graphs of the course of friction coefficient values in relation to the distance and time for chosen samples T0, T0,7 and T0,9 for friction force velocity 1.1 [m/s], and load 175 [N].

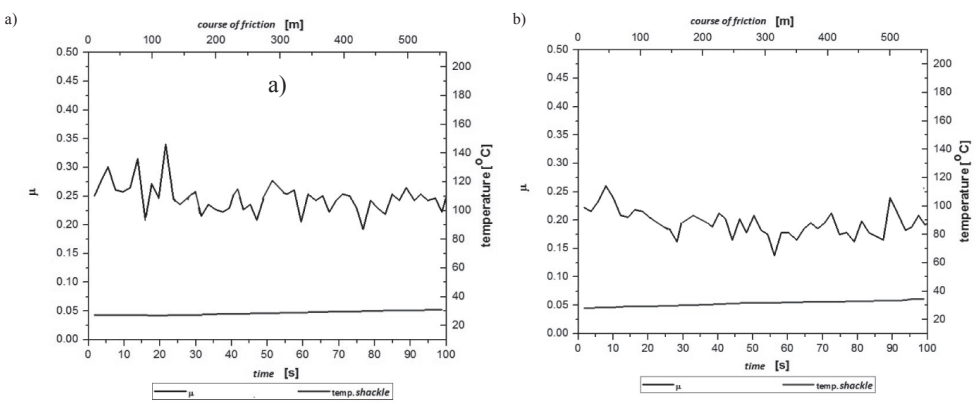


**Fig. 6. Diagram of the course of friction coefficient in relation to the distance and time for friction speed 1.1 [m/s], load 175 [N]: a) sample T0, - μs = 0.247, b) sample T0,7- μs = 0.194**
Rys. 6. Wykres przebiegu wartości współczynnika tarcia w funkcji drogi i czasu dla prędkość sił tarcia 1,1 [m/s], obciążenie 175 [N]: a) próbka T0, - μs = 0.247, b) próbka T0,7 -μs = 0,194

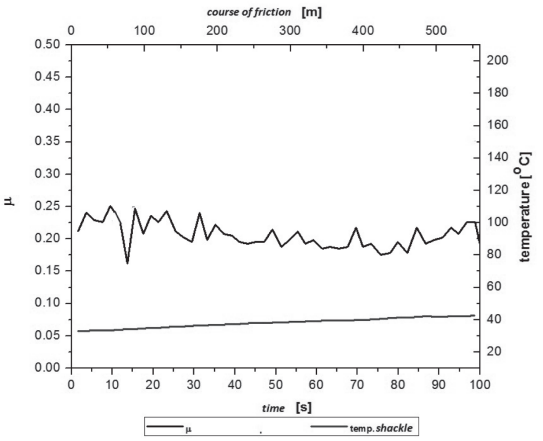


**Fig. 7. Diagram of the course of friction coefficient as a function of distance and time for sample T0,9, friction rate 1.1 [m/s], load 175 [N] - μs = 0.206**

Rys. 7. Wykres przebiegu wartości współczynnika tarcia w funkcji drogi i czasu dla próbki T0,9 prędkość sił tarcia 1.1 [m/s], obciążenie 175 [N] - μs = 0,206

Analysis of the courses of friction rate coefficient and temperatures shown in **Figure 8** prove the absence of the phenomenon of adhesive wear and scuffing. Moreover, thanks to the used additional sensors such as accelerometers and a microphone, after FFT (Fast Fourier transform) analysis of the tested research runs, it was proven that the obtained results are reliable and can be used in quantity and quality evaluations of the effects of the developed technology. **Figure 8** presents a histogram of FFT analysis of vibration acceleration values in three axes (tangential, transverse, and vertical) and the sound level of selected measuring gear of the sand conditioned and unconditioned samples.

With the purpose of the quantification of the durability increase on the basis of tribological tests, the relative durability of the roller's surface was calculated. Relative durability due to friction wear was described by the following dependency (3):

$$T_{EK} = \frac{T_{ekk}}{T_o} \cdot 100\% \tag{3}$$

where

$T_{ekk}$ – roller's surface durability, made according to a newly developed technology,

$T_o$ – roller's surface durability produces at present (referential one).

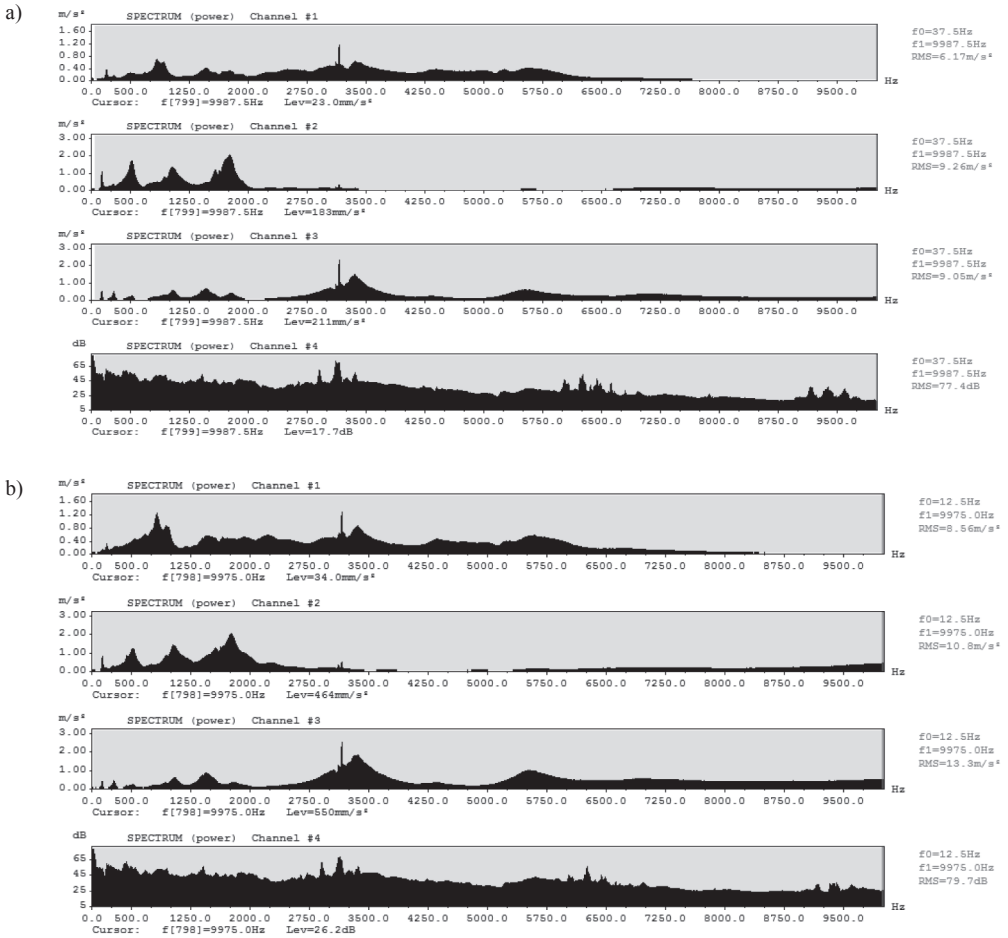


**Fig. 8. Histogram of FFT analysis of vibration acceleration values in three axes (tangential, transverse, and vertical) and the sound level of selected measuring gear: a) sand conditioned sample, b sample unconditioned in sand**

Rys. 8. Histogram analizy FFT wartości przyspieszeń drgań, w trzech osiach: stycznej, poprzecznej i pionowej oraz poziomu dźwięku z wybranego biegu pomiarowego: a) próbka kondycjonowana w pisaku, b) próbka niekondycjonowana w piasku

Relative durability values calculated on the basis of tribological tests and using dependency (3) are shown in **Fig. 9**.

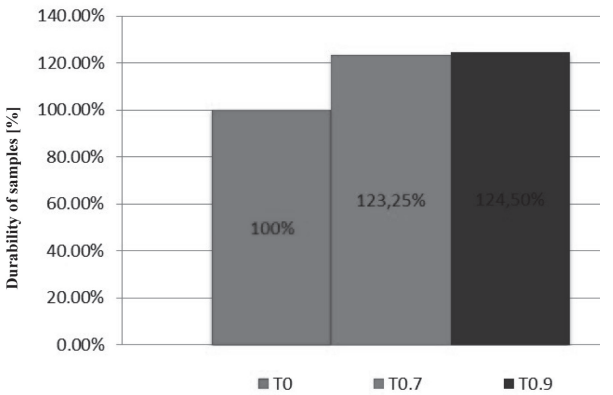


**Fig. 9. Histogram of relative durability in percentage for tested tribological samples T0, T0.7, T0.9**

Rys. 9. Histogram trwałości względnej w ujęciu procentowym dla badanych tribologicznie próbek T0, T0.7, T0.9

The state of knowledge on the abrasive wear resistance of metals, available in science publications on tribology **[L. 4, 6, 7]** and resulting from the authors' research experience in the field of tribological exploitation of the rail vehicle elements allows making the following statement: Abrasive wear resistance of different metals, and especially steel grades of various structures in each of the analysed cases is different, yet in each of these particular cases abrasive wear resistance is proportional to their hardness. Thus, the product of relative abrasion resistance of a metal and its hardness is a constant value for a given metal family. Therefore, by analogy, it was accepted that, for the same steel abrasive wear, resistance is proportional to the hardness and especially to the micro-hardness and it was described by the following dependency (4):

$$J_{WZ\_S235} \cdot H = \text{const} \tag{4}$$

where

$J_{WZ\_S235}$ – relative friction wear resistance of the roller's surface made of S235 steel,

$H$ – micro-hardness of S235 steel HV 0.01.

The possibility of predicting the abrasive wear resistance of the roller's surface made of S235 steel after applying dynamic burnishing technology is presented in **Fig. 10**.

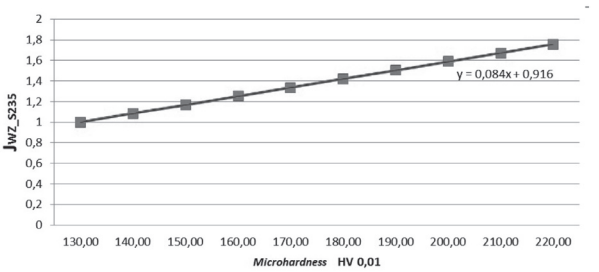


**Fig. 10. Graph of the model prediction of relative abrasive wear resistance $J_{WZ\_S235}$ of a roller surface made of S235 steel as a function of micro hardness HV 0.01 on cross-section**

Rys. 10. Wykres przebiegu predykcji modelowej względnej odporności na zużycie ścierne płaszcza krążnika wykonanego ze stali S235

The above model refers to a realized comparative experiment. In real conditions, the model of the tribological node does not include the metal–abrasive and metal–resin contact, e.g., in the form of dust. Thus, based on experience in the actual exploitation of tribological systems with metal–resin contact, a beneficial effect of wear limiting will be significantly better. It can be forecast that, with advantageous synergy of the external factors, the total durability of the roller subjected to shot peening technology will be, due to abrasive wear, 100% higher than a roller not subjected to peening.

## CONCLUSION

Compressive stresses are advantageous for increasing fatigue strength and reducing cracking resulting from stress corrosion, hydrogen embrittlement, fretting corrosion, seizing, and erosion caused by cavitation as well as fatigue cracking within the zone of thermal influence. Compressive stresses formed due to shot peening reach the maximum value right under the surface of the roller surface. The values of compressive stresses reach about half of the proof stress of S235 steel. Therefore, significant reduction of these unfavourable wear types is also forecast. However, the final verification requires carrying out, among others, exploitation tests in order to verify the accepted assumptions to predict durability and the reliability of the plain steel roller surface made of S235 steel in the energy effective and innovative technology of increasing fatigue strength developed by the authors.

**REFERENCES**

1. Hebda H.,Wachal A.: Trybologia, WNT, Warszawa 1980.
2. Katsuji T.: Papers on shot peening published in the world for the last thirteen years, The 7th INTERNATIONAL CONFERENCE ON SHOT PEENING, Instytut Mechaniki Precyzyjnej, Warszawa, 1999.
3. Nakonieczny A.: Powierzchniowe obróbki wyrobów metalowych Instytut Mechaniki Precyzyjnej, Warszawa, 2000.
4. Nachman G.: Shot peening – past, present and future, The 7th INTERNATIONAL CON-FERENCE ON SHOT PEENING, Instytut Mechaniki Precyzyjnej, Warszawa, 1999.
5. Nakonieczny A.: Dynamiczna powierzchniowa obróbka plastyczna kulowaniem, Instytut Mechaniki Precyzyjnej, Warszawa 2002.
6. Noury P., Eriksson K.: Failures of high strength stainless bridge roller bearings, Engineering Fracture Mechanics, vol. 180, July 2017, pp. 315–329.
7. Berto F., Campagnolo A., Chebat F., Cinera M., Santini M.: Fatigue strength of steel rollers with failure occurring at the weld root based on the local strain energy values, International Journal of Fatigue, vol. 82, part 3, January 2016, pp. 643–657.